OSU

The Ohio State University

RESONANT REGION NCTR RESEARCH

E.K. Walton
F.D. Garber
D.L. Moffatt
J.D. Young

The Ohio State University

ElectroScience Laboratory

Department of Electrical Engineering
Columbus, Ohio 43212

Semi-Annual Report 718048-1
Contract No. N00014-86-K-0202
July 1986

Department of the Navy
Office of Naval Research
800 N. Quincy St.
Arlington, VA 22217-5000

NOTICES

When Government drawings, specifications, or other data are used for any purpose other than in connection with a definitely related Government procurement operation, the United States Government thereby incurs no responsibility nor any obligation whatsoever, and the fact that the Government may have formulated, furnished, or in any way supplied the said drawings, specifications, or other data, is not to be regarded by implication or otherwise as in any manner licensing the holder or any other person or corporation, or conveying any rights or permission to manufacture, use, or sell any patented invention that may in any way be related thereto.

50272-101

REPORT DOCUMENTATION PAGE	1. REPORT NO.	2.	3. Recipient's Accession No.

4. Title and Subtitle

Resonant Region NCTR Research

5. Report Date
July 1986

6.

7. Author(s)
E.K. Walton, F.D. Garber, D.L. Moffatt, J.D. Young

8. Performing Organization Rept. No.
718048-1

9. Performing Organization Name and Address
The Ohio State University ElectroScience Laboratory
1320 Kinnear Road
Columbus, Ohio 43212

10. Project/Task/Work Unit No.

11. Contract(C) or Grant(G) No
(C) N00014-86-K-0202
(G)

12. Sponsoring Organization Name and Address
Department of the Navy
Office of Naval Research
800 N. Quincy St.,
Arlington, VA 22217-5000

13. Type of Report & Period Covered

14.

15. Supplementary Notes

16. Abstract (Limit: 200 words)

This report discusses progress being made in research on resonant region radar target identification. Topics studied include the use of Complex Natural Resonances (CNR's), syntactic-classifier-based identification techniques, optimization criteria for feature selection, and target substructure studies.

Under the topic of Complex Natural Resonances (CNR), classification probability results using the Lai model are shown for the case of two commercial aircraft. Predictor-correlator results are also shown for a set of three land vehicles.

In the case of syntactic target identification, an analysis of the performance of three different pattern representation schemes has been begun. Level and octant crossing examples have been used with the OSU/ESL data base to derive a set of syntactic primitives. Studies are given showing the classification performance for the three types of primitives derived here. This area of research has also begun the development of a feature vector optimization scheme based on various cost functions. Results are given.

The study of substructure identification based on transient waveforms and polarimetric color images has also begun to produce results. Some preliminary conclusions are given in Chapter V on this topic.

17. Document Analysis a. Descriptors

Radar Target Identification
Complex Natural Resonances
Radar Cross Section

b. Identifiers/Open-Ended Terms

c. COSATI Field/Group

Accession For	
NTIS GRA&I	☒
DTIC TAB	☐
Unannounced	☐
Justification	
By	
Distribution/	
Availability Codes	
Dist	Avail and/or
A-1	

18. Availability Statement
A. Approved for Public Release; distribution is unlimited.

19. Security Class (This Report) Unclassified

21. No. of Pages 57

20. Security Class (This Page) Unclassified

22. Price

(See ANSI-Z39.18) See Instructions on Reverse OPTIONAL FORM 272 (4-77) (Formerly NTIS-35) Department of Commerce

TABLE OF CONTENTS

LIST OF TABLES

LIST OF FIGURES

I. INTRODUCTION

This report discusses progress on Resonant Region NCTR research being conducted at The Ohio State University under sponsorship of the Office of Naval Research (contract no. N00014-86-K-0202). This project builds upon past research in which an advanced far-field microwave measurement range (The Ohio State University Compact Range) was developed for the experimental measurement of the resonant region scattering signatures of modern ships, aircraft and ground vehicles [1-11].

The development of this scattering measurement range and the systems and subsystems required for the operation of such a range was followed by an extensive measurement program. The RCS of a number of modern ships, aircraft, and ground vehicles as a function of frequency, polarization, elevation angle, and azimuth angle was measured. The data gathered was organized into a file-oriented data base with cross referenced header systems and a data base management system. The radar targets included in this data base and the frequency bands utilized are tabulated in Table 1.1.

This data base is recognized as one of the most comprehensive and accurate RCS data bases in the world today. Other organizations have been interested in using these data for research into radar target identification. It has been shared with a number of laboratories in the United States. Below is a list of the other users of these data.

TABLE 1.1

1983-1985 ELECTROSCIENCE LABORATORY

RESONANCE REGION DATA BASE - ONR No. N00014-82-K-0037

Target	Scale	Frequency
Boeing 747	200	5-60 MHz
Boeing 707	150	6.7-80 MHz
Boeing 727	200	5-60 MHz
DC-10	200	5-60 MHz
Concorde	130	7.7-92 MHz
USS Long Beach	500	4-36
Cimarron Class Fleet Oiler	500	4-36
Trinidad Cargo Ship	450	4.4-50 MHz
Ship Set (6)		
Small scale	2400	0.8-7.5 MHz
Larger scale	1200	0.8-15 MHz
Ground Vehicle (5) 3 tanks, 1 truck, 1 jeep	87	23-207 MHz

Note: some data available for the aircraft in higher frequency bands.

TABLE 1.2

OTHER USERS OF THE OSU RESONANT REGION RCS DATA BASE

Dr. Robert Dinger	Naval Weapons Center, China Lake, CA
Dr. V.K. Jain	University of S. Florida, Tampa, FL
Prof. Wolfgang Boerner	Dept. of Electrical Engineering, University of Illinois, Chicago, IL

Note that in the tapes sent to these users, the names of the targets are designated by sequence numbers, and the users of these data do not have access to those names without the express release of such names by the ONR.

The Ohio State University will continue to provide copies of the data base to other institutions as directed by the ONR.

In previous years, the OSU ElectroScience Laboratory has had considerable success in the development and testing of concepts and algorithms for radar target classification and identification using this data base. Details of these developments can be found in the many reports, M.Sc. theses and Ph.D. dissertations produced under sponsorship of these programs [3, 4, 6, 8, 10, 11].

This research is divided into a number of specific tasks as listed below.

1. Target recognition algorithm development

   a. Complex natural resonance studies
   b. Decision theoretic classification

2. Testing against real world targets

3. Propagation characteristic model testing

4. Extension of the previously developed techniques to target substructures.

Each of these areas are discussed below.

II. TARGET RECOGNITION ALGORITHM DEVELOPMENT

A. Target Identification using Complex Natural Resonances

The purpose of this section of the report is to detail the progress which has been made in the development of methods for the identification of targets from radar signals using the complex natural resonances (CNR's) of the targets. Two major problem areas are covered, extraction of CNR's from measured scattering data for a target and application of these CNR's in prediction-correlation and other procedures for target identification.

CNR Extraction

Every finite object can be characterized electromagnetically by an infinite set of singularities which are poles of some finite order [12]. This has only been proven for finite conducting objects, but the extension to dielectric and composite bodies would seem a reasonable assumption. In practice, the assumption of simple poles and a finite number of singularities is usually made. When the vector wave equation is separable, transcendental equations for the CNR's can be derived. This has been done for spherical objects (conducting and dielectric) but not for the conducting disc. For electrically small objects, the CNR's can be obtained from an integral equation formulation and numerical search. For the geometrically complicated object of more than very modest electrical size the only recourse is extraction of the CNR's from either measured scattering data or from measured surface current densities.

When an aperiodic excitation illuminates a body, the far zone response is characterized by first a forced response as the wavefront moves over the body and then a free or natural response as the wavefront moves beyond the body. If a time domain model is to be used for CNR extraction then it is necessary to delay in time until the response is a free response. One might postulate time-dependent residues and apply the model to the entire waveform but, as pointed out by Felson [13], this would require very great numerical precision.

In the frequency domain (complex) the early time problem is manifested by the presence of an entire function. Therefore in the frequency domain a model for extracting CNR's must at least partially take into account the presence of an entire function contribution to the data. We favor a frequency domain approach to CNR extraction because for a complicated (geometrically) target many substructures may resonate and decay long before the wavefront moves beyond the target. Therefore there would be no chance of extracting these CNR's. For uncomplicated structures one can clearly separate forced response and free response. For complicated structures; however, beyond very short times the response is a very complicated combination of forced response and free response and a clear time separation is not possible.

In a recent dissertation by Lai [14], an approximate frequency domain model with a first order estimate to include the entire function was tested. By using a rational function model with a numerator polynomial of order one greater than the denominator polynomial it is possible to include a constant term and a term linear with frequency

both of which have unknown coefficients. This is the same as adding an impulse and doublet with unknown weights at the time origin of a time domain model. Actually a more general model was postulated which included phase shifts (time delays) but to use this model and still generate linear equations for the coefficients the time delays would have to be estimated from a measured band-limited impulse repsonse. The coefficients are, of course, orientation and frequency dependent. A summary of this work was published [15], and it will also be included in a report in preparation which will summarize all of our CNR extraction and target identification results [16].

Certain results obtained using the Lai model [14] are shown in Tables 2.1, 2.2, and 2.3. Tables 2.1 and 2.2 show the extracted poles (oscillatory part only) of two commercial aircraft. The aircraft were good electroplated models and the measured scattering data spanned the model frequency range 1.0 to 6.0 GHz. The models were physically about the same size but have different scale factors. Table 2.3 shows the complex poles of both aircraft after averaging over the measured angles. Vertical polarization was used for these measurements with the wings of the aircraft in a horizontal plane. An angle of zero degrees corresponds to nose-on incidence. As seen in the tables, a crude estimate of the entire function does permit excitation invariant oscillatory parts of poles to be extracted from meaningful measured data on realistic aircraft models. Unfortunately, the real parts of the complex poles shown in Table 2.3 are not meaningful in the sense of target identification. That is, poor correlation ensues if the poles

TABLE 2.1

IMAGINARY PART OF POLES

OF AIRCRAFT A AT VARIOUS ANGLES

	0°	10°	20°	30°	60°	90°	120°	150°	180°	Ave.
(1)	1.181	1.171	1.134	1.204	1.103	1.143	1.125	1.121	1.096	1.142
(2)	1.280	1.299	1.309	1.352	1.270	1.372	1.475	1.292	1.423	1.341
(3)	1.589	1.622	1.560	1.608	1.572	1.602	1.798	1.560	1.650	1.618
(4)	2.002	1.985	1.945	1.946	1.990	1.911	2.067	1.942	1.893	1.965
(5)	-----	-----	2.386	2.405	2.256	2.205	2.267	2.326	2.217	2.295
(6)	2.527	2.501	2.634	-----	-----	2.491	2.576	2.593	2.493	2.545
(7)	2.777	2.792	2.859	2.861	2.838	2.739	2.791	2.790	2.750	2.800
(8)	3.190	3.137	3.177	3.076	3.272	3.262	3.023	3.159	3.235	3.170
(9)	3.532	-----	3.375	3.417	3.481	3.466	3.446	-----	-----	3.453
(10)	3.843	3.632	3.666	3.797	-----	3.851	3.821	3.619	3.733	3.745
(11)	4.183	4.222	4.167	4.210	4.224	4.329	4.272	4.186	-----	4.224
(12)	4.472	4.737	4.431	4.510	4.615	4.659	-----	4.500	4.632	4.570

TABLE 2.2

IMAGINARY PART OF POLES

OF AIRCRAFT B AT VARIOUS ANGLES

	0°	15°	30°	60°	90°	120°	150°	180°	Ave.
(1)	1.051	1.047	1.034	-----	-----	1.070	-----	1.098	1.060
(2)	1.345	1.311	1.348	1.321	1.354	1.381	1.373	1.365	1.350
(3)	1.611	1.747	1.635	1.536	1.575	1.663	1.620	1.627	1.627
(4)	1.995	2.039	1.920	1.944	2.028	2.055	1.994	2.017	1.999
(5)	2.293	2.160	2.332	2.253	2.257	2.375	2.344	2.402	2.302
(6)	2.663	2.635	2.503	2.647	2.615	2.578	2.666	2.549	2.607
(7)	2.995	3.005	2.841	3.073	3.021	2.958	2.893	2.972	2.970
(8)	3.320	3.345	3.321	3.384	3.320	3.238	3.231	-----	3.308
(9)	3.732	3.691	3.738	-----	-----	3.639	-----	3.507	3.661
(10)	4.036	4.182	-----	3.955	4.151	3.995	-----	-----	4.064
(11)	4.663	-----	4.394	4.739	4.482	4.510	4.551	4.549	4.555

TABLE 2.3

POLES OF AIRCRAFTS A AND B

AVERAGED OVER THE MEASURED ANGLES

A	B
(1) -.121 + j 1.142	(1) -.151 + j 1.060
(2) -.214 + j 1.341	(2) -.190 + j 1.350
(3) -.216 + j 1.965	(3) -.215 + j 1.627
(4) -.157 + j 1.965	(4) -.175 + j 1.999
(5) -.162 + j 2.295	(5) -.144 + j 2.302
(6) -.137 + j 2.545	(6) -.174 + j 2.607
(7) -.098 + j 2.800	(7) -.193 + j 2.970
(8) -.154 + j 3.170	(8) -.217 + j 3.308
(9) -.157 + j 3.453	(9) -.184 + j 3.661
(10) -.235 + j 3.745	(10) -.160 + j 4.064
(11) -.205 + j 4.224	(11) -.170 + j 4.555
(12) -.180 + j 4.570	

in Table 2.3 are applied to the actual measured data. It would be possible of course to use the poles in Table 2.3 to obtain an approximate scattering model by solving for the residues at each measured angle. Prediction-correlation applied to the approximate scattering model would then yield excellent identification results and would be excitation invariant. In our opinion, this type of procedure would yield unrealistic conclusions with regard to predition-correlation target identification. The variance of the real part of the poles dictates that either the target orientation must be known or that each target must be treated as several targets as discussed in the section on target identification using CNR's.

The Lai dissertation [14,17] also demonstrated that when the scattering data are dominated by specular-type contributions then there is real merit in the use of cross-polarized scattering data even though the cross-polarized response may be 10 to 15 dB down from the co-polarized returns. This work was partially supported on a companion contract N00014-84-K-0705. CNR's were extracted for four incidence angles (the aircraft orientation is as described above) using three polarizations, vertical-vertical, horizontal-horizontal, and vertical-horizontal. The extracted CNR's (oscillatory parts only) are shown in Table 2.4. Table 2.4 shows that while no incidence angle yields all of the CNR's, the cross-polarized results have a lower rate of absenteeism than the co-polarized results. In the region near broadside (ninety degrees) a great deal of processing was required to extract the co-polarized CNR's but very little was needed with the cross-polarized

returns. There is little specular-type returns in the cross-polarized data. This fact makes the cross-polarized returns much easier to process for CNR extraction.

We have concluded that the measured data for CNR extraction must come from controlled measurements, i.e., from measurements on a good compact range such as the one at the ElectroScience Laboratory. It is not feasible at this stage to consider CNR extraction from noisy full scale scattering data. Our approach to target identification then requires an à priori library of CNR's for the targets of interest. These CNR's need not necessarily be the dominant CNR's of the structure (CNR's with smallest oscillatory parts) but will generally be at lower frequencies since as more and more substructures on the structure resonate the density of pole locations will become prohibitive for target identification purposes. Lai [14,17] also demonstrated this by extracting CNR's from measured data taken over a model frequency span of 6.0 to 12.0 GHz. The CNR's remained orderly, i.e., an excitation invariance was obtained for the oscillatory part of the poles. These results illustrate that it is feasible to consider target identification using CNR's of particular substructures rather than the dominant CNR's.

Target Identification

The prediction-correlation algorithm for target identification uses à priori CNR's of the target from a library and samples of a measured unknown target spectrum to obtain a calculated spectrum which is then compared (correlation) to the unknown target spectrum. The method is roughly the same as that given in [18], with a change in normalization

TABLE 2.4

OSCILLATORY PARTS OF CNR'S
EXTRACTED FROM BACKSCATTER RESPONSES
OF DIFFERENT POLARIZATIONS AND ANGLES FOR AIRCRAFT C

0°			45°			90°			180°		
VV	VH	HH	VV	VH	HH	VV	VH	HH	VV	VH	HH
-----	1.143	1.017	1.215	1.134	1.106	1.259	1.050	1.090	1.208	1.198	1.100
1.408	1.470	1.474	1.494	1.574	1.626	1.427	1.490	-----	1.473	1.488	1.439
1.642	1.682	1.770	1.765	1.797	-----	1.714	1.821	1.742	-----	-----	-----
-----	1.956	1.958	1.919	-----	2.097	-----	2.015	2.128	2.097	2.038	1.926
2.330	2.195	2.280	2.210	2.247	2.418	2.420	-----	-----	2.298	2.341	2.233
2.720	2.512	2.592	2.657	2.656	2.717	-----	2.647	2.643	2.657	-----	2.597
-----	2.905	3.073	2.965	2.871	-----	2.947	3.065	-----	3.047	2.870	-----
3.310	3.287	-----	3.298	3.271	3.276	3.349	-----	-----	-----	3.321	3.219
3.586	3.747	3.654	-----	3.707	3.675	-----	3.639	3.781	3.645	3.572	-----
4.026	4.059	4.159	3.893	4.067	-----	3.971	4.103	4.113	4.100	4.021	4.145
4.192	4.239	-----	-----	-----	4.208	-----	-----	-----	4.226	4.241	-----
-----	4.718	4.543	4.627	4.727	4.684	4.717	4.671	-----	4.596	-----	4.510
-----	-----	5.056	-----	5.024	5.136	-----	-----	-----	-----	4.924	4.796
5.442	5.505	5.533	-----	-----	-----	5.51	5.547	5.511	-----	5.677	5.622

and other changes dictated by the nature of the extracted CNR's. Both CNR extraction and the identification algorithm are evolving processes and therefore the identification results are not exhaustive, i.e., not all targets and not all available measured scattering data have been tested.

Prediction-correlation identification results for two naval vessels were reported in a thesis by Jalloul [19]. Jalloul's results did not have the first order estimate of the entire function and the extracted CNR's show more variation in their oscillatory parts than would now be the case. A summary of the results obtained by Jalloul is shown in Figures 1 and 2. These figures give the probability of classification of each ship as a function of aspect (bow-on is zero degrees) with the noise to signal ratio as a parameter. The measurements were made at an elevation angle of 30 degrees with the ships on a ground plane. Both figures show that in the vicinity of 20 degrees from bow-on classification probability is rather poor. For one ship (the OL) classification was also poor for stern-on. The results shown in Figures 1 and 2 were obtained using aspect-varying optimization parameters. That is, the actual spectral range and pole locations were chosen to optimize the correlation between calculated and measured spectrums for the noise free case. Therefore to use the library, either the ship orientation would have to be known or the ship treated as some 9 different targets. It is interesting to observe that the ship's orientation could be estimated using this approach. This research revealed one weakness of the prediction-correlation algorithm which was

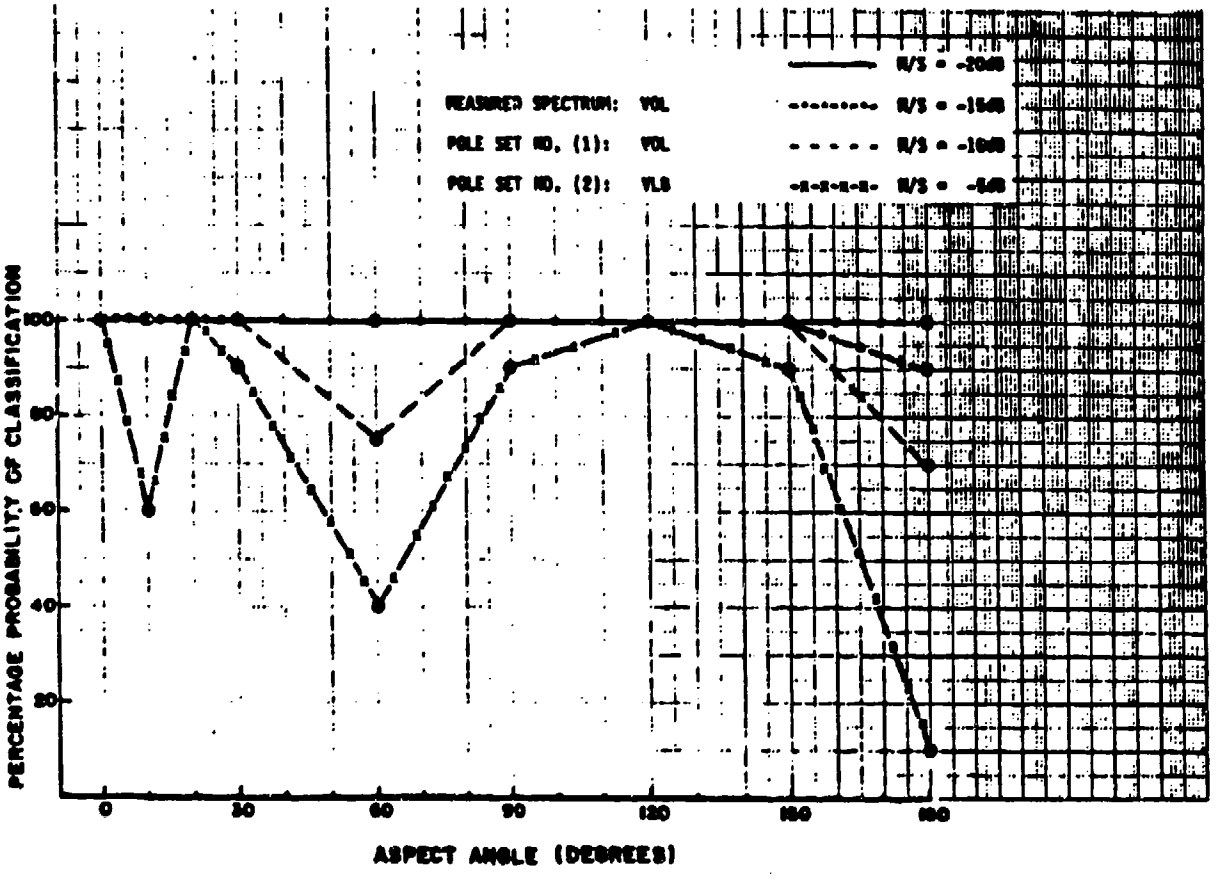

Figure 1. Classification probability curves versus aspect angle for the indicated noise-to-signal ratios. These plots show the probability of classification of target "OL" when the spectrum of "OL" is measured given two possible targets "OL" and "LB".

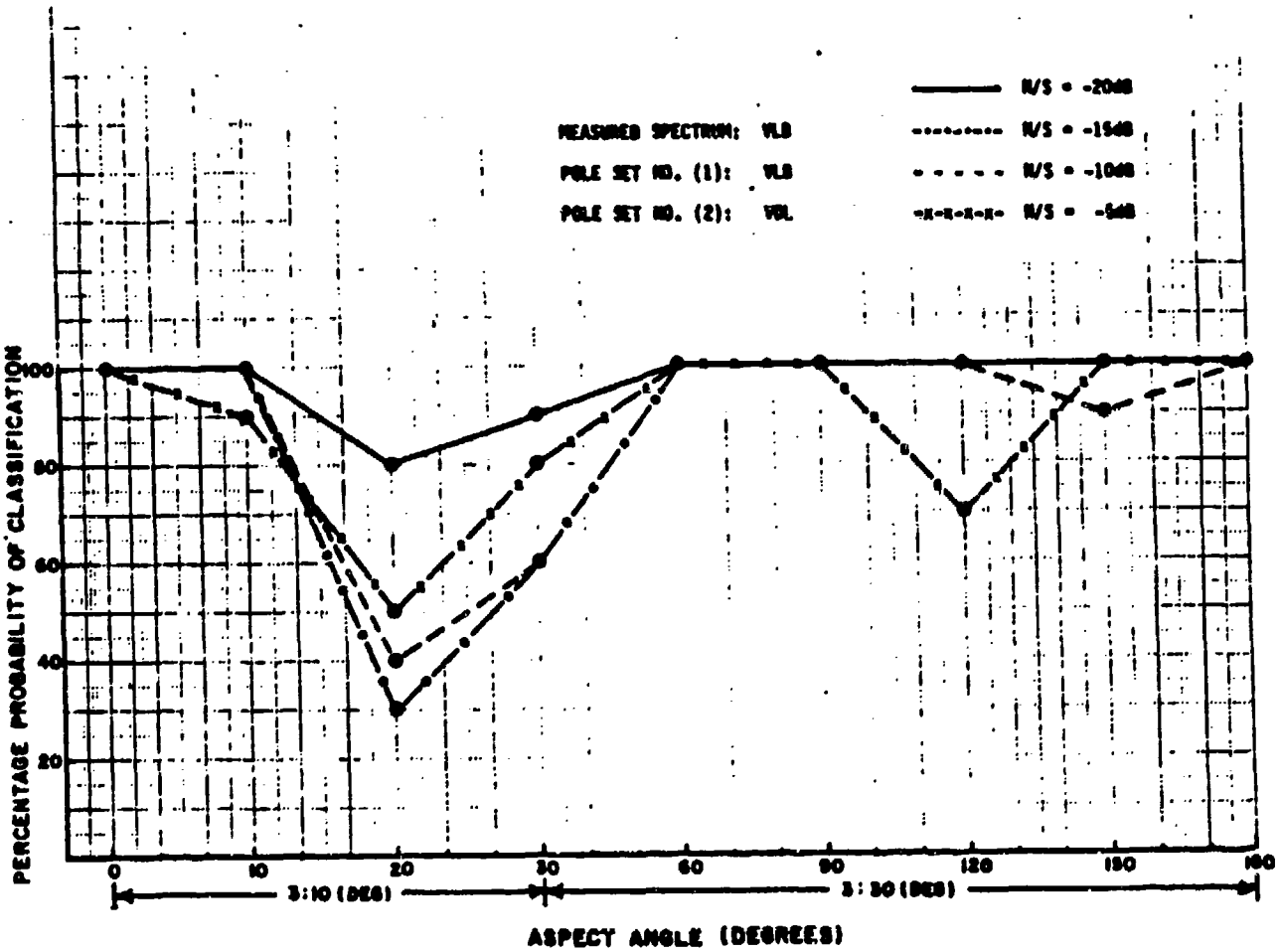

Figure 2. Classification probability curves versus aspect angle for the indicated noise-to-signal ratios. These plots show the probability of classification of target "LB" when the spectrum of "LB" is measured given two possible targets "OL" and "LB". (The horizontal axis has two different scales as indicated.)

later reinforced by identification tests with other targets. The predicted waveform is really a residue series and if too many poles are used then the residues can adjust to match almost any spectrum. Therefore in practice, no more than 10 to 12 pole pairs can be used.

The prediction-correlation algorithm was applied to three commercial aircraft targets by Moffatt and Barkeshli [20]. This paper was prepared for a NATO/AGARD Target Signature Symposium but was withdrawn at the request of the sponsoring agency for classification reasons. It also did not appear in the classified Conference Proceedings. These initial results did not utilize the entire function estimate and the frequency span used was not optimized with respect to aspect. The orientation of the aircraft and the angle interpretation are as described previously. Because the scale factors for the aircraft targets were not the same, it was necessary to scale to the full scale frequencies (10.0 to 30.0 MHz) which were used for all tests. It was found that for aspects near nose-on, good classification results could be obtained but the results were erratic. These results dictated the need for improvements in the model (entire function) and in optimization as a function of aspect.

The predictor-correlator algorithm was also tested on a set (3) of land vehicles. The scattering measurements were made at an elevation angle of 30 degrees with the targets on a ground plane. The model frequencies were 2.0 to 18.0 GHz. In this case the model used to extract CNR's included the estimate of the entire function and the parameters were optimized with respect to aspect. Typical

classification probabilities are shown in Figure 3. A 90 degree aspect in this case corresponds to broadside incidence. These results and others were given in a thesis by Bohley [21].

The entire function estimation procedure introduced by Lai [14], can also be used as a different target identification algorithm. In this approach, the CNR's and entire function parameters are first obtained as described before. Next a prescribed amount of pseudo-random noise is added to the scattering data and the entire function parameters carefully obtained. For modest amounts of noise (S/N of 15 dB at the moment) these parameters are sufficiently stable to permit target identification. Figure 4 shows the results of this approach for the identification of three commercial aircraft. The aircraft orientation is as previously described, wings of the aircraft are in a horizontal plane and zero degrees corresponds to nose-on incidence, and vertical polarization was used for the results in Figure 4. This algorithm has the disadvantage that noise must be added to the data to estimate the parameters. Also, stabilization of the parameters for lower signal to noise ratios is not a simple problem.

Recent developments on a companion program (Contract No. N00014-78-C-0049) described in a dissertation by Fok [22] dictate that the K-pulse target identification algorithm be briefly described. The K-pulse is a unique interrogating waveform of minimal duration which elicits time-limited response waveforms from a target for all aspects and polarizations. The K-pulse is excitation invariant but the response waveforms are aspect and polarization dependent. Previous methods for

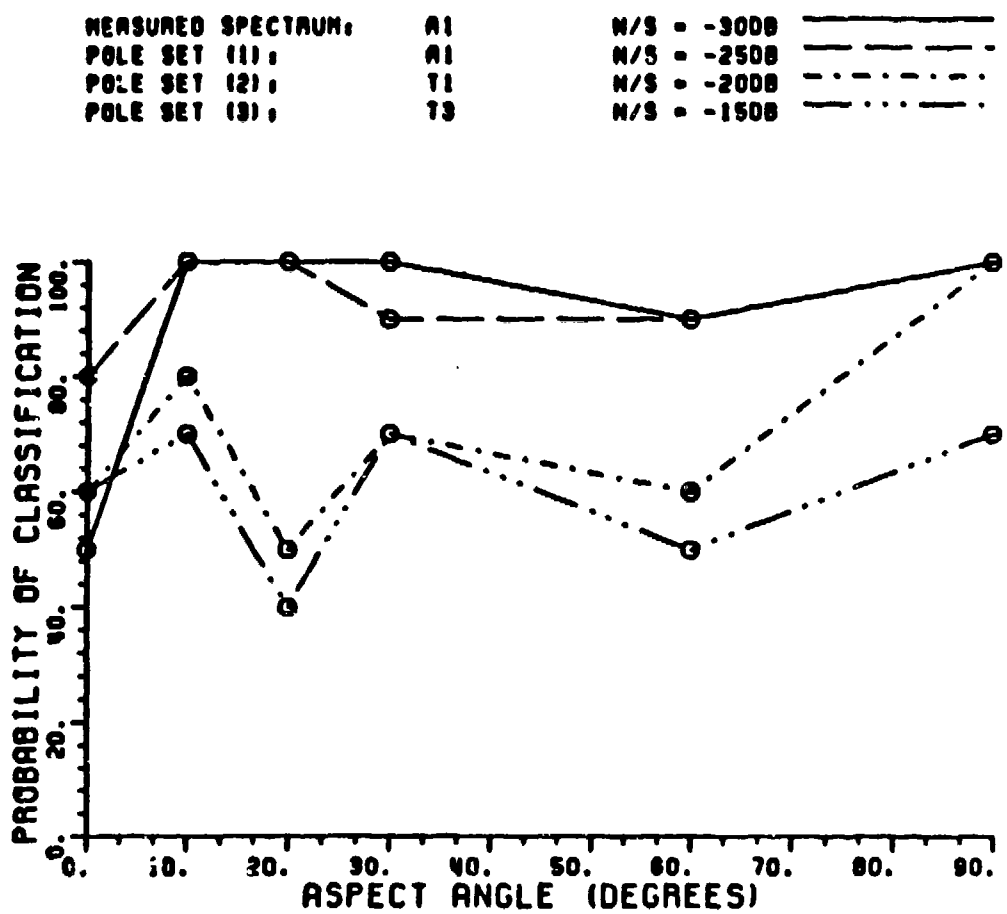

Figure 3. Probability of classification versus aspect angle for target A1. This set of curves indicates the probability of classifying target A1, for the indicated noise-to-signal ratios, from the pole sets of targets T1, T3, and A1.

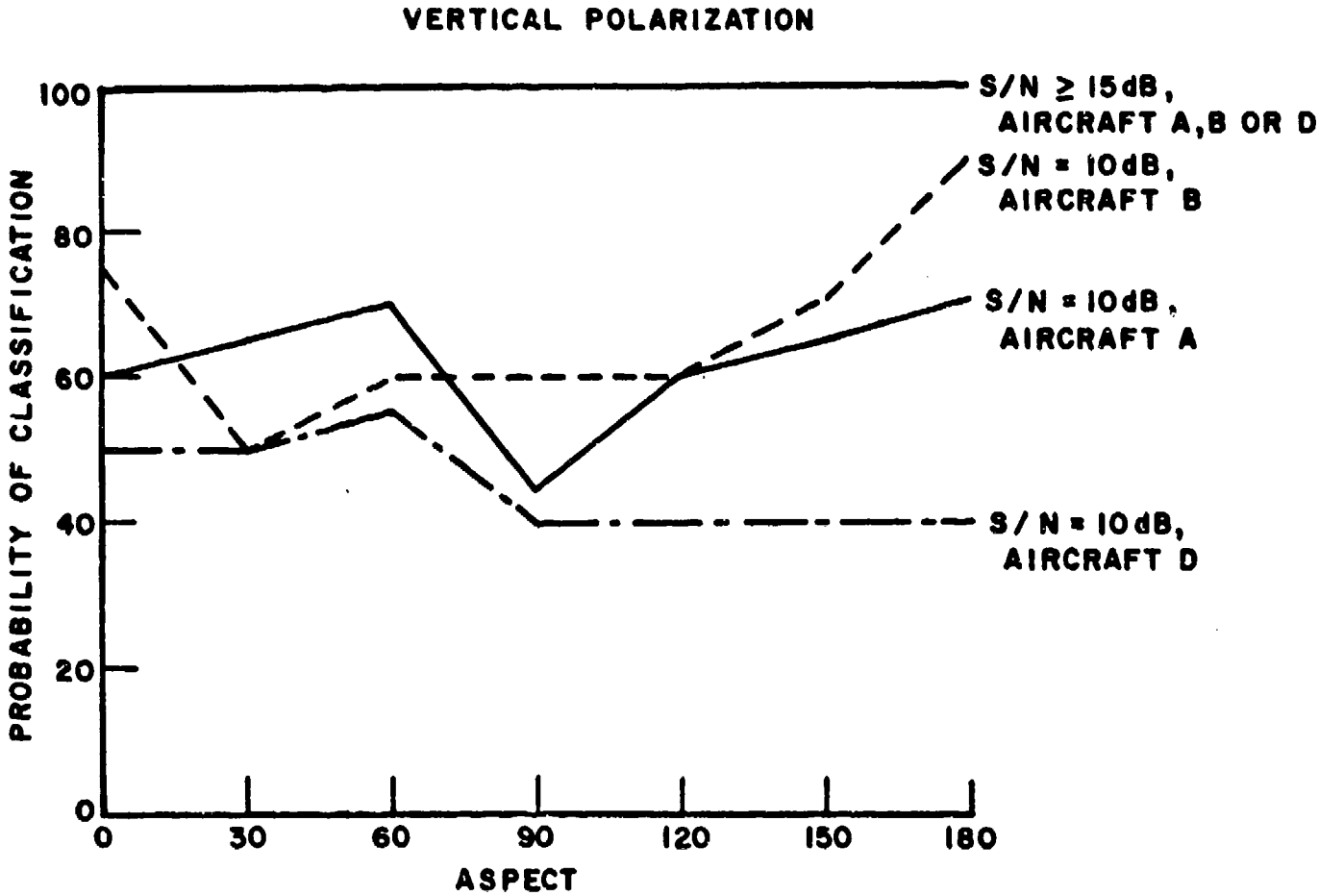

Figure 4. Probability of classification vs. aspect angle for target A1. This set of curves indicates the probability of classifying target A1, for the indicated noise to signal ratios, from the pole sets of targets T1, T3 and A1.

obtaining the K-pulse required knowledge of at least some of the CNR's of the target. Given the non-stability of the real part of the CNR's extracted from scattering data on realistic targets, the K-pulse would be aspect-dependent. Now however the technique described by Fok generates a K-pulse estimate without knowledge of the target's CNR's. Therefore a scheme whereby a measured broadband scattered signal is passed in parallel through a bank of K-pulse filters corresponding to the targets of interest is indeed feasible. The measured targets scattering data must first be processed to dilute the effect of both high and low frequencies. Efforts in this direction are in progress. K-pulses have been generated for a grounded dielectric slab, a wire, a loop, a disc, a sphere and a finite length circular waveguide. For complicated targets such as those of interest on this program, K-pulses for particular substructures of the target may be more desirable.

III. DEVELOPMENT AND EVALUATION OF SYNTACTIC-CLASSIFIER-BASED RADAR TARGET IDENTIFICATION SYSTEMS

A. Introduction

As a part of the present research program, we have been investigating the applicability of syntax-based pattern recognition to radar target identification. In particular, we have been developing and testing computer simulation packages that can be used to determine the feasibility and evaluate the performance of syntactic pattern recognition radar target identification systems.

Traditionally, classification methods based upon decision-theoretic concepts have been applied to the radar target identification problem. The historic popularity of decision theoretic applications is primarily due to the well-defined sense of optimality for these schemes. Our own research concerning decision-theoretic techniques indicates that these schemes are especially appropriate when target measurements are represented as elements in a vector space.

The syntactic approach to pattern recognition classifies a pattern representation of a radar target measurement by means of a structural description of the pattern [23, Chapter 1]. This is in sharp contrast to the parametric, feature-based description of target measurements employed by decision-theoretic methods. In syntactic pattern recognition systems, an analogy is drawn between the structure of the symbolic target description (discussed below) and the syntax of an inferred grammatical system. The capability of providing a structural description of the measurement pattern may prove to be of significant utility for the radar target identification problem. This is especially

significant when the number of classes is large, or when the number of target and catalog measurements is such that the classification task becomes impractical to implement. In addition, it is felt that a structural description may provide useful information about the target; even in cases when the system is unable to classify the target as a member of the available catalog.

B. Classifier Formulation

A syntactic radar target identification system may be viewed as consisting of a pattern representation section, which processes the return signal measurements into a symbolic description of the target, and a syntax analysis section which uses the symbolic description to deduce the identity of the unknown target. The first step in developing a syntactic radar target identification strategy is to formulate a pattern representation scheme appropriate for both the target set of interest as well as the envisioned radar system. The pattern representation scheme should be designed so as to correspond to the geometrical characteristics of the target. The process of generating such a representation primarily consists of converting a radar cross-section measurement waveform (pattern) to a string of symbols called primitives. The resulting primitives characterize local portions of the cross-section waveform (or target); the complete string of symbols thus represents the entire waveform (target).

The discrete nature of the pattern representation symbols is required for the operation of the syntax analysis section of the radar target identification system. The organization of these symbols into

symbol strings, on the other hand, is not necessary for implementation of a syntactic classifier. Indeed, previous investigations of symbol assignments for measurement waveforms indicate that higher dimensional pattern representations would allow more reliable classification [24]. Notwithstanding, this method of organization of pattern representation symbols is carried out in order to simplify the resulting algorithm for this preliminary study.

It is clear, from an information-theoretic standpoint, that the development of a pattern representation scheme is the most crucial part of the specification of a syntactic radar target identification system. The representation scheme must preserve information that is sufficient for identification. That is, the statistic formed by the pattern representation must be sufficient to identify the target.

Theoretically, it is always possible to find a pattern representation that is sufficient static. Indeed, such a system could be implemented by combining a pattern representation scheme that is an analog of a decision-theoretic classification system with a syntactic classifier that is merely an identity mapping (i.e., simply announce the representation symbol). However, prior to this investigation, there existed considerable doubt that a practical pattern representation scheme could be developed that contained statistics sufficient for reliable identification of radar targets: the sufficiency of practical symbolic pattern representations for the identification of aircraft radar targets is the primary focus of this study.

As is the case for the evaluation of other key performance parameters of practical target identification systems, the analytical evaluation of the sufficiency of the various pattern representation schemes, and hence the performance of the target classification system, is extremely difficult and cumbersome. Thus, the sufficiency of the statistic formed by a pattern representation scheme is implicitly evaluated by means of a Monte-Carlo simulation, which compiles results on the performance of the syntactic target identification system when applied to simulated radar returns in additive noise.

The primary function of the syntax analysis section of the system is to identify the target. This task is implemented as likelihood-ratio tests using likelihood functions or approximations of likelihood functions. The formulation of each likelihood function is, in general, dependent on the characteristics of the noise. Hence, the decision rule formed by these likelihood functions is optimal (given the pattern representation), only for the noise level for which the functions are obtained. However, it is believed that the ordering induced on the pattern representations by the likelihood functions remains unchanged for different noise levels so that likelihood ratio test should exhibit some robustness in performance with respect to changes in the power level of the noise.

Since, in practice, likelihood functions are difficult to fully characterize, they are approximated, in our study, by computing relative frequency densities for the symbol patterns. The approximate densities are formed by generating a fixed number (50 in the examples discussed

below) of simulated noisy radar returns for a particular target, processing these waveforms into pattern representations, and computing the relative frequency of appearance for each observed pattern. A second set of relative frequencies is then generated by repeating the process, and the two estimates of the densities are compared. If the two density estimates are similar, the estimate is used, otherwise, the process continues until a suitable estimate for the true density is found.

1. Pattern Representation Schemes

In order to gain insight into the effects of the pattern representation on the performance of syntactic target identification, we have evaluated the performance of systems using three different pattern representation schemes. Each of these represents a radar return measurement in terms of "level crossings." This type of representation was, in part, suggested by the results as reported [25] and [26] which indicated that much of the information contained in a waveform is also contained in its zero crossings. Moreover, pattern representations of the level-crossing type realize other properties that are intuitively desirable. For example, in order to reduce the complexity of the syntax analysis section of the classifier, the set of primitives (or symbols) necessary to represent a given pattern should be as small as possible. In addition, the pattern representation processing subsystem should be easy to implement, and the resulting representations should be relatively immune to the effects of noise. Each of the pattern representation schemes discussed below exhibit one or more of these desired characteristics.

Single Level Crossing

The single level crossing pattern representation is based on the formulation of primitives that correspond to the number of consecutive (in frequency) radar return measurements that lie above or below a pre-determined threshold. The first of these primitives is the number of consecutive measurements, of the initial set of measurements, having magnitude below the threshold. In case the first measurement lies above the threshold, the first primitive is taken to be zero. The second primitive is the number of consecutive measurements, subsequent to the intial set, that have magnitude above the threshold; and so on until all the measurements in the set have been accounted for. Note that the only place a zero can occur is in the first position of the string of primitives.

The pre-determined threshold for this scheme is taken to be the average value of the magnitude of the measurement data. Thus, the threshold must be between the minimum and maximum values of magnitudes of the measurement waveforms. Also notice that the size of the set of primitives for this scheme is not fixed and varies with the number of measurements taken by the system. An example of the single level crossing processing technique is shown in Figure 5.

Octant Crossing with Redundancy Removal

The octant crossing method of pattern representation incorporates the simplicity of level crossing determination into a scheme that also employs partial phase information. The representation algorithm begins by calculating the average value of the magnitude of the measurement

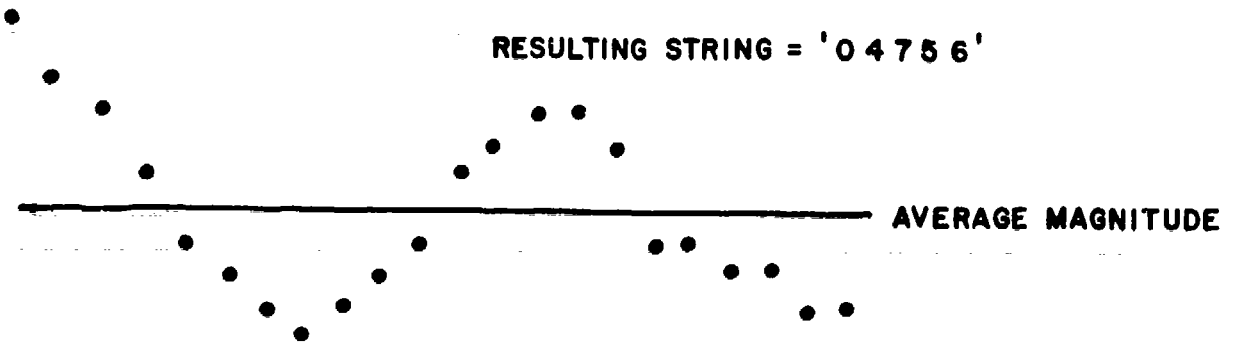

Figure 5. Single level crossing representation example.

data to determine the threshold level. During operation, the radar receiver decides whether the measurement has magnitude above or below this threshold, and, in addition, the "quadrant" in which the measurement lies is calculated. The resulting octant of a radar measurement for each combination of level and quadrant is defined by the following table. The categories "above" and "below" refer only to the magnitude of the measurement while the phase ranges refer only to the angle. As in the double level crossing case discussed below, the redundant (repeated) primitive appearing in a representation string are removed.

In the octant representation scheme, the number of primitives is eight so that the syntax analysis section of the classifier is easy to implement. Moreover, the implementation of this processing technique is a straightforward extension of the single level crossing algorithm.

Table 3.1

OCTANT PRIMITIVE ASSIGNMENTS

Octant	Phase	Magnitude
a	0-90	below
b	90-180	below
c	180-270	below
d	270-360	below
e	0-90	above
f	90-180	above
g	180-270	above
h	270-360	above

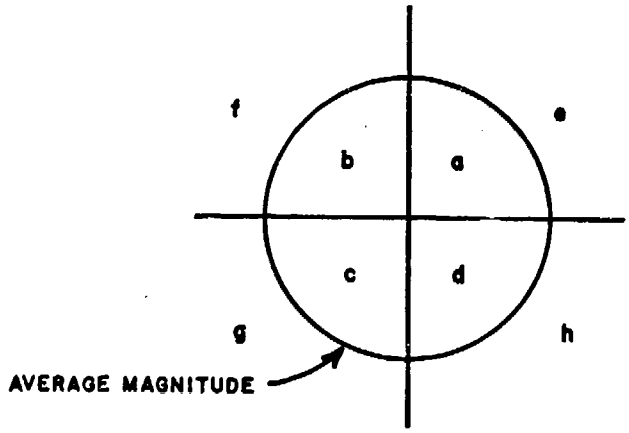

Table 3.2

DOUBLE LEVEL CROSSING PRIMITIVE ASSIGNMENTS

Level	Magnitude
a	below lower threshold
b	above lower threshold, below upper threshold
c	above upper threshold

Double Level Crossing with Redundancy Removal

The double level crossing method of pattern representation begins by determining the maximum and minimum magnitudes of the radar measurements of interest. Upper and lower thresholds are then chosen so as to divide the measurement range into thirds. During operation, primitives are assigned to the observed measurements according to their position relative to these two thresholds as shown in Table 3.2. Finally, redundant symbols are removed from the pattern representation string by deleting primitives that repeat.

Since the number of primitives for the double level crossing representation scheme is smaller than either of the other schemes, it is expected that this latter scheme may be least affected by noise and interference. Actual implementation of this technique requires little more complexity than the single level crossing scheme.

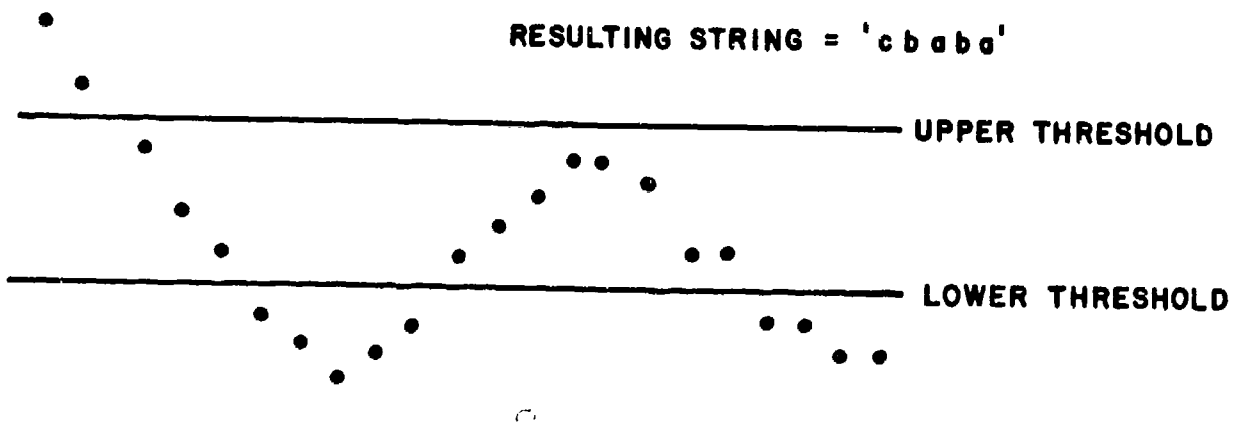

Figure 6. Double level crossing representation example.

C. Results

The following tables contain the results of simulation experiments performed on the syntactic radar target identification systems discussed above applied to a catalog consisting of the radar cross section measurements of 5 aircraft targets, each measured at 0° azimuth and 0° elevation, for 11 equally spaced frequencies in the range from 8 MHz to 58 MHz, at HH polarization. The results were compiled for 500 Monte-Carlo experiments for each aircraft.

Table 3.3

AVERAGE MISCLASSIFICATION PERCENTAGES VS. NOISE LEVEL:

DOUBLE LEVEL CROSSING REPRESENTATION

Design Noise Level (dBm^2)	Test Noise Level									
	2.00	5.00	10.00	11.00	12.00	13.00	14.00	15.00	20.00	25.00
5	0.20	1.16	11.44	14.48	18.92	24.56	31.60	38.16	71.40	92.04
10	0.20	1.04	6.80	13.92	13.92	18.16	21.20	28.36	63.76	86.20
15	0.12	1.20	7.28	10.48	12.44	12.44	14.96	18.60	45.32	73.56

Table 3.4

AVERAGE MISCLASSIFICATION PERCENTAGE VS. NOISE LEVEL:

OCTANT CROSSING REPRESENTATION

Design Noise Level (dBm^2)	Test Noise Level									
	2.00	5.00	10.00	11.00	12.00	13.00	14.00	15.00	20.00	25.00
5	0.04	1.72	23.16	32.32	41.52	50.84	62.44	70.64	96.36	99.88
10	0.00	0.00	4.80	10.12	16.72	25.36	38.28	47.80	90.96	99.56

Table 3.5

AVERAGE MISCLASSIFICATION PERCENTAGES VS. NOISE LEVEL:

SINGLE LEVEL CROSSING REPRESENTATION

Design Noise Level (dBm^2)	Test Noise Level									
	2.00	5.00	10.00	11.00	12.00	13.00	14.00	15.00	20.00	25.00
5	2.84	5.32	19.68	24.16	30.32	35.12	44.12	50.00	77.92	94.60
10	8.36	6.40	6.60	8.20	9.84	12.72	16.68	21.08	57.20	84.96
15	8.36	6.60	5.80	6.08	6.48	8.16	9.36	11.84	37.28	69.80

C. Results

The following tables contain the results of simulation experiments performed on the syntactic radar target identification systems discussed above applied to a catalog consisting of the radar cross section measurements of 5 aircraft targets, each measured at 0° azimuth and 0° elevation, for 11 equally spaced frequencies in the range from 8 MHz to 58 MHz, at HH polarization. The results were compiled for 500 Monte-Carlo experiments for each aircraft.

Table 3.3

AVERAGE MISCLASSIFICATION PERCENTAGES VS. NOISE LEVEL:

DOUBLE LEVEL CROSSING REPRESENTATION

Design Noise Level (dBm^2)	Test Noise Level									
	2.00	5.00	10.00	11.00	12.00	13.00	14.00	15.00	20.00	25.00
5	0.20	1.16	11.44	14.48	18.92	24.56	31.60	38.16	71.40	92.04
10	0.20	1.04	6.80	13.92	13.92	18.16	21.20	28.36	63.76	86.20
15	0.12	1.20	7.28	10.48	12.44	12.44	14.96	18.60	45.32	73.56

Table 3.4

AVERAGE MISCLASSIFICATION PERCENTAGE VS. NOISE LEVEL:

OCTANT CROSSING REPRESENTATION

Design Noise Level (dBm^2)	Test Noise Level									
	2.00	5.00	10.00	11.00	12.00	13.00	14.00	15.00	20.00	25.00
5	0.04	1.72	23.16	32.32	41.52	50.84	62.44	70.64	96.36	99.88
10	0.00	0.00	4.80	10.12	16.72	25.36	38.28	47.80	90.96	99.56

Table 3.5

AVERAGE MISCLASSIFICATION PERCENTAGES VS. NOISE LEVEL:

SINGLE LEVEL CROSSING REPRESENTATION

Design Noise Level (dBm^2)	Test Noise Level									
	2.00	5.00	10.00	11.00	12.00	13.00	14.00	15.00	20.00	25.00
5	2.84	5.32	19.68	24.16	30.32	35.12	44.12	50.00	77.92	94.60
10	8.36	6.40	6.60	8.20	9.84	12.72	16.68	21.08	57.20	84.96
15	8.36	6.60	5.80	6.08	6.48	8.16	9.36	11.84	37.28	69.80

Table 3.6

AVERAGE MISCLASSIFICATION PERCENTAGES VS. NOISE LEVEL

FOR VARIOUS PATTERN REPRESENTATION SCHEMES

(DESIGN NOISE LEVEL = 10 $dBsm^2$)

Scheme	Test Noise Level 2.00	5.00	10.00	11.00	12.00	13.00	14.00	15.00	20.00	25.00
Double	0.20	1.04	6.80	9.72	13.92	18.16	21.20	28.36	63.76	86.20
Octant	0.00	0.00	4.80	10.12	16.72	25.36	38.28	47.80	90.96	99.56
Single	8.36	6.40	6.60	8.20	9.84	12.72	16.68	21.08	57.20	84.96

D. Conclusions

These results show that the pattern representation schemes described in this report preserve sufficient information to reliably identify each of the radar targets in the catalog tested. Future investigations in this area will focus on the implementation of the syntax analysis section of the identification system as well as the development of more general pattern representation schemes. Particular emphasis will be placed on the identification of pattern representation schemes that explicitly correspond to target superstructures and substructures so that the role of syntax analysis may be expanded to include a target description in addition to target identification.

IV. RECENT RESULTS ON THE SELECTION AND EXTRACTION OF FEATURES FOR RADAR TARGET IDENTIFICATION

A. Introduction

In this report, we briefly describe some of the recent work conducted in the ElectroScience Laboratory at The Ohio State University that is focused on the extraction and selection of features from a large, multi-dimensional data set. The feature extraction process typically involves the formulation of an optimal linear transformation from the original n-dimensional measurement space to an orthogonal k-dimensional feature space, where $k \leq n$. Each element (or feature) in the transformed space is thus a linear combination of elements (measurements) in the measurement space. It is desirable that the linear transformation is chosen to minimize a cost function that is closely related to the average probability of classification error, though, in practice, such a cost function may be difficult to formulate.

In feature selection, the objective is to identify a set of k features that minimize a cost function, just as for feature extraction. However, in this case, the chosen features are in one-to-one correspondence with the measurements. Thus, while the feature extraction process produces a set of k features, each of these may be a combination of possibly many measurements. The goal of feature selection is to obtain performance as reliable as with feature extraction; while requiring only a fixed, modest number of measurements.

As a part of this investigation, the resulting performance of both methods is evaluated by means of Monte-Carlo simulation using the data base and simulation software described in [27].

B. Transformation and Cost Criteria

During the initial phase of this study, an optimized linear transformation based on an algorithm discussed in [28], was chosen and a criteria function described in [29] was employed. This transformation maps the measurement space into an orthogonal feature space in which the extracted features are uncorrelated.

The first step in formulating this transformation is to compute the intra-class covariance matrix for each class of targets. The inter-class covariance matrix is then computed for this same collection of classes. The transformation discussed above is chosen such that the average intra-class covariance matrix becomes the identity matrix in the orthogonal feature space; and the inter-class covariance matrix is a diagonal matrix. That is, in the feature (range) space, the average intra-class covariance is the same in any direction and the features are uncorrelated.

The eigenvalues and the eigenvectors of the intra-class and the inter-class co-variance matrices have a direct bearing on the obtainable system performance. In particular, the eigenvalues of the inter-class covariance matrix (under the constraint that the average intra-class covariance matrix is identity), gives in indication of how well the classes separate in the direction of the corresponding eigenvectors. The larger these eigenvalues are, the better the classes separate in

that direction. As an example, assume we found that the sum of the largest k eigenvalues is nearly equal to the sum of the remaining n-k eigenvalues. This would imply that the target classes have significant separation only in the direction of the k corresponding eigenvectors but do not show significant separation in the direction of any of the other n-k eigenvectors. This, in turn, would imply that little could be gained by attempting to classify this set of targets in any space with more than k dimensions.

As stated before, the disadvantage of optimal feature extraction is that the extracted features are linear combinations of possibly many measurements in the original space. In order to overcome the inherent disadvantage of feature extraction discussed above, we have examined procedures by which exhaustive searches for the optimal set of k measurements can be implemented, where optimality is based on the same cost criterion discussed above.

C. Initial Results

Feature extraction and feature selection based on the methods described above were applied to sets of data (HHP) for 5 commercial aircraft at 0° elevation. The radar cross section for each aircraft was measured at 19 different azimuth angles (from 0° to 180°), in 1 MHz steps in the 8 MHz to 58 MHz range. Thus, in this case, the dimension of the measurement space is 51, the number of prototypes for each class is 19 and the number of classes is 5.

After applying the feature extraction criteria, it was observed that only 4 eigenvalues of the inter-class covariance matrix were of

significant value so that the transformation matrix to the orthogonal feature space consisted of the 4 corresponding eigenvectors; reducing the dimension of the classification problem from 51 to only 4. The resulting classification error was less than 20 (magnitude-only) measurements.

By applying feature selection criteria to obtain an optimum set of frequencies, it was observed that the optimum 3, the optimum 5, and the optimum 8 frequencies, etc., do not provide as reliable classification as if all 51 frequency measurements are used. On the other hand, it was observed that the performance advantage available with increasing the number of measurements in this frequency band quickly becomes less significant.

D. Modified Cost Criteria Functionals

While the initial performance results for the feature extraction and feature selection techniques discussed above exhibited substantial performance gains for the HHP data catalog set, the corresponding results for the VHP catalog set were not as encouraging. Indeed, for certain tests employing the VHP catalog data, the feature selection algorithm identified a set of frequency measurements that produced worse results than an arbitrary choice of equally spaced frequencies.

The primary reason for this initial disappointment is the fact that the feature selection technique discussed above does not exhibit a direct relationship to the resulting probability of classification error. Rather, the motivation for this technique is based on the concept of "distance" in the feature space; a parameter that influences,

but does not determine the error probability for multiple, composite hypothesis testing problems such as the one considered in the present study.

A number of alternatives to the "maximum-distance" feature extraction and selection criteria are currently under investigation. The first of these, which places more significance on prototypes (target catalog entries) most likely to be confused, and less significance on prototypes that are unlikely to be misclassified, is based on the weight function

$$w(\xi_i^l,\xi_j^k) = \exp\left\{\frac{\sum_{m=1}^{M}(\xi_j^l(m)-\xi_j^k(m))^2}{2\sigma^2}\right\} \qquad (1)$$

where $\xi_j^l(m)$ is the i^{th} prototype of class 1 measured at frequency m. The feature selection criteria is then formed for any desired number of measurements M as

$$J = \sum_{l=1}^{L-1}\sum_{k=l+1}^{L}\sum_{i=1}^{n_i}\sum_{j=1}^{n_j}\exp\left\{\frac{\sum_{m=1}^{M}(\xi_j^l(m)-\xi_j^k(m))^2}{2\sigma^2}\right\}$$

$$= \sum_{l=1}^{L-1}\sum_{k=l+1}^{L}\sum_{i=1}^{n_i}\sum_{j=1}^{n_j} w(\xi_i^l,\xi_j^k) \qquad (2)$$

Notice that this feature selection criteria function is an exponentially-weighted sum of the more commonly employed Euclidean distance metric between prototypes belonging to distinct classes. Thus, if two prototypes are dissimilar, they are assigned a weight ≈ 1, indicating a high probability of the two targets being confused.

Alternatively, if two prototypes from distinct classes are not similar, they are assigned a weight ≈ 0 corresponding to a low probability of misclassification for this pair. The feature selection process then procedes by identifying a set of M measurements that minimize the criterion in (2), i.e.,

$$J_{opt} = \min_{M} J$$

The factor, σ^2, appearing in (1) is used as a normalization to match the noise power level likely to be encountered. This factor affects the resulting weight function by adjusting the measure of similarity of prototypes according to the magnitude of the expected measurement errors due to noise.

The results of simulation studies of the performance of radar target identification systems based on this feature selection criterion are shown in Table 4.1 for HHP catalog data, and in Table 4.2 for VHP catalog data. Graphical displays of these results appear in Figure 7 for the HHP catalog data and in Figure 8 for the VHP catalog data. These results indicate that the modified feature selection criterion is successful in achieving more reliable classification performance than the Euclidean distance discriminant criteria function (or arbitrary, equally spaced frequency selection), especially for noise levels near the design noise power level.

Table 4.1

SIMULATED CLASSIFICATION RESULT OF THE OPTIMUM SET OF 4 FREQUENCIES FOR VARIOUS FEATURE SELECTION ALGORITHMS USING THE HHP DATA

The first column contains the noise level, but the others the misclassification percentage at the given noise level. The average power at the features selected in each case is given above the corresponding column.

For:

Pave = 26.02 dBsm discriminant criteria function
Pave = 26.30 dBsm equally spaced frequencies (1,17,34,51)
Pave = 26.59 dBsm exponential weighting function at 10 dBsm
Pave = 26.49 dBsm exponential weighting function at 20 dBsm
Pave = 27.18 dBsm exponential weighting function at 30 dBsm

dBsm	26.02	26.30	26.59	26.49	27.18
0.00	0.00	0.00	0.00	0.00	0.00
2.00	0.00	0.00	0.00	0.00	0.00
4.00	0.00	0.00	0.00	0.00	0.00
6.00	0.00	0.00	0.00	0.00	0.00
8.00	0.00	0.11	0.00	0.00	0.00
10.00	0.42	0.53	0.00	0.00	0.11
12.00	0.63	1.58	0.21	0.21	0.32
14.00	2.74	2.63	0.42	0.74	0.95
16.00	4.32	7.79	1.89	1.37	3.37
18.00	11.58	16.11	6.42	6.32	9.47
20.00	20.74	24.53	14.95	14.11	15.37
22.00	31.16	35.47	24.00	22.95	27.79
24.00	40.74	46.42	37.79	36.32	38.21
26.00	47.79	54.63	49.89	47.58	48.00
28.00	57.58	60.11	56.74	55.37	55.26
30.00	63.89	66.42	64.32	63.68	59.68
32.00	68.63	70.53	68.74	69.58	67.58
34.00	73.37	72.74	71.47	71.47	72.53
36.00	72.95	73.68	74.63	76.21	76.53
38.00	74.21	76.21	74.21	75.89	77.58
40.00	79.26	77.47	76.74	77.68	76.74
42.00	74.63	78.21	78.95	79.37	77.58
44.00	78.32	79.47	78.42	79.26	78.53
46.00	79.16	77.37	80.74	78.32	77.79
48.00	79.47	79.26	80.00	80.53	77.47
50.00	77.37	80.42	80.63	81.47	80.42

Table 4.2

SIMULATED CLASSIFICATION RESULT OF THE OPTIMUM SET OF 4 FREQUENCIES FOR VARIOUS FEATURE SELECTION ALGORITHMS USING THE VHP DATA

The first column contains the noise level, but the others the misclassification percentage at the given noise level. The average power at the features selected in each case is given above the corresponding column.

For:

Pave = 20.74 dBsm discriminant criteria function
Pave = 18.53 dBsm equally spaced frequencies (1,17,34,51)
Pave = 19.07 dBsm equally spaced frequencies (4,19,33,48)
Pave = 14.97 dBsm exponential weighting function at 0 dBsm
Pave = 20.63 dBsm exponential weighting function at 10 dBsm
Pave = 21.03 dBsm exponential weighting function at 20 dBsm

dBsm	20.74	18.53	19.07	14.97	20.63	21.03
-10.00	0.00	0.00	0.00	0.00	0.00	0.00
- 8.00	0.00	0.11	0.11	0.00	0.00	0.11
- 6.00	0.53	0.21	0.21	0.00	0.11	0.42
- 4.00	0.53	0.21	0.53	0.00	0.11	0.63
- 2.00	0.63	0.53	1.05	0.00	0.42	1.68
0.00	1.79	0.95	1.79	0.42	0.53	2.32
2.00	2.95	1.47	2.74	1.16	2.00	3.68
4.00	4.84	3.37	4.21	3.26	2.95	5.05
6.00	8.00	4.21	6.53	6.74	3.58	5.68
8.00	14.11	8.42	10.00	12.53	6.11	8.32
10.00	18.95	13.26	12.74	20.95	8.74	9.68
12.00	24.84	20.95	21.26	34.95	15.37	14.32
14.00	33.05	28.32	24.11	42.63	21.16	19.47
16.00	38.74	34.42	35.89	50.11	28.63	27.68
18.00	48.42	47.47	46.11	60.42	38.74	34.63
20.00	52.74	55.68	52.47	68.32	45.89	42.53
22.00	58.84	58.42	57.79	69.05	54.32	52.42
24.00	64.21	68.63	65.68	72.42	60.21	60.74
26.00	66.84	71.47	69.26	76.84	65.58	68.21
28.00	70.63	73.89	74.84	75.58	69.58	69.37
30.00	70.84	74.74	71.37	77.58	74.11	73.26
32.00	75.47	76.32	74.74	78.84	74.21	76.42
34.00	75.58	78.53	76.00	79.58	76.42	74.84
36.00	77.68	79.89	77.26	78.95	76.74	77.16
38.00	76.95	79.79	78.00	77.68	76.32	75.37
40.00	77.89	79.79	78.00	77.05	78.74	76.42

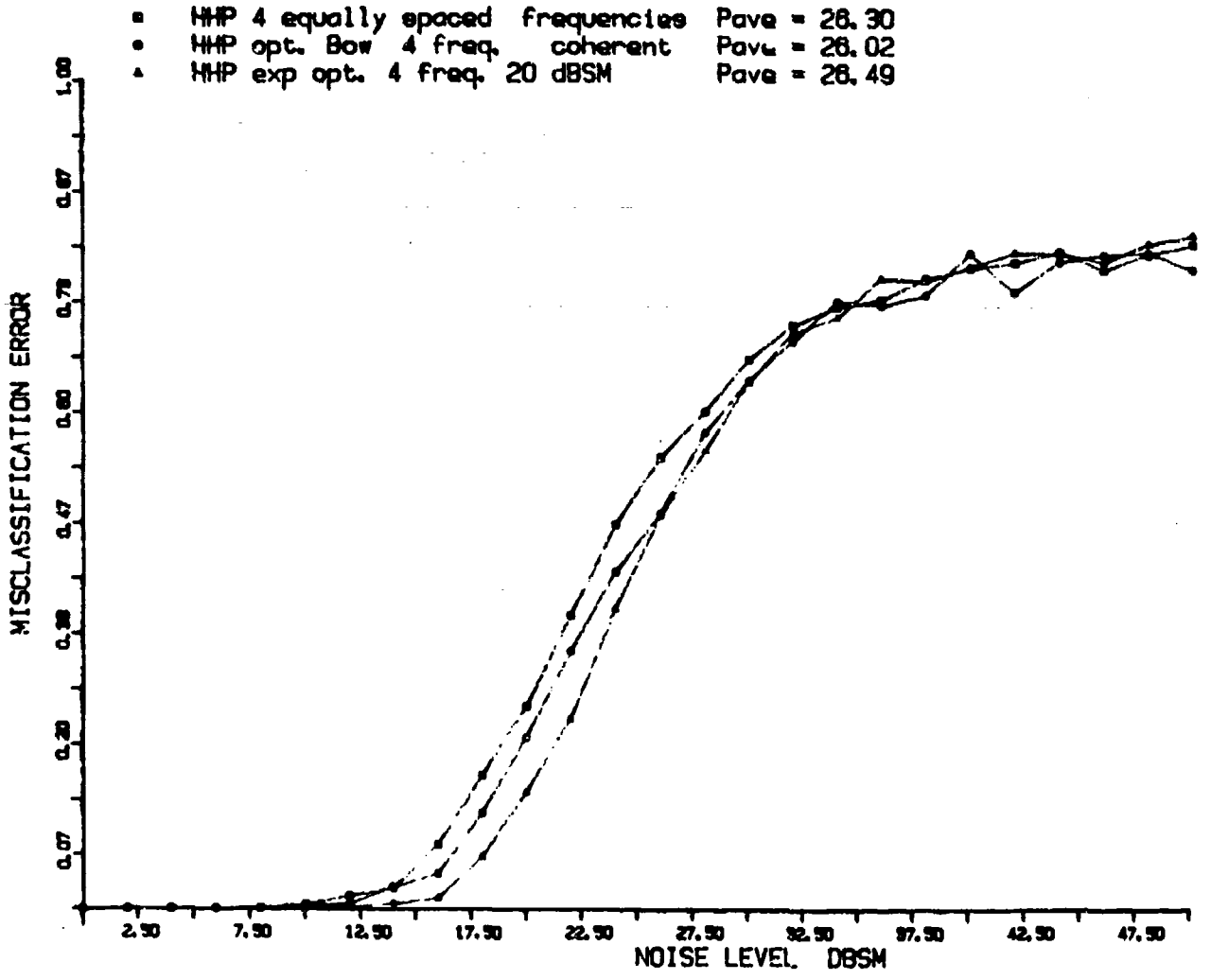

Figure 7. Misclassification error as a function of noise level (HHP catalog data).

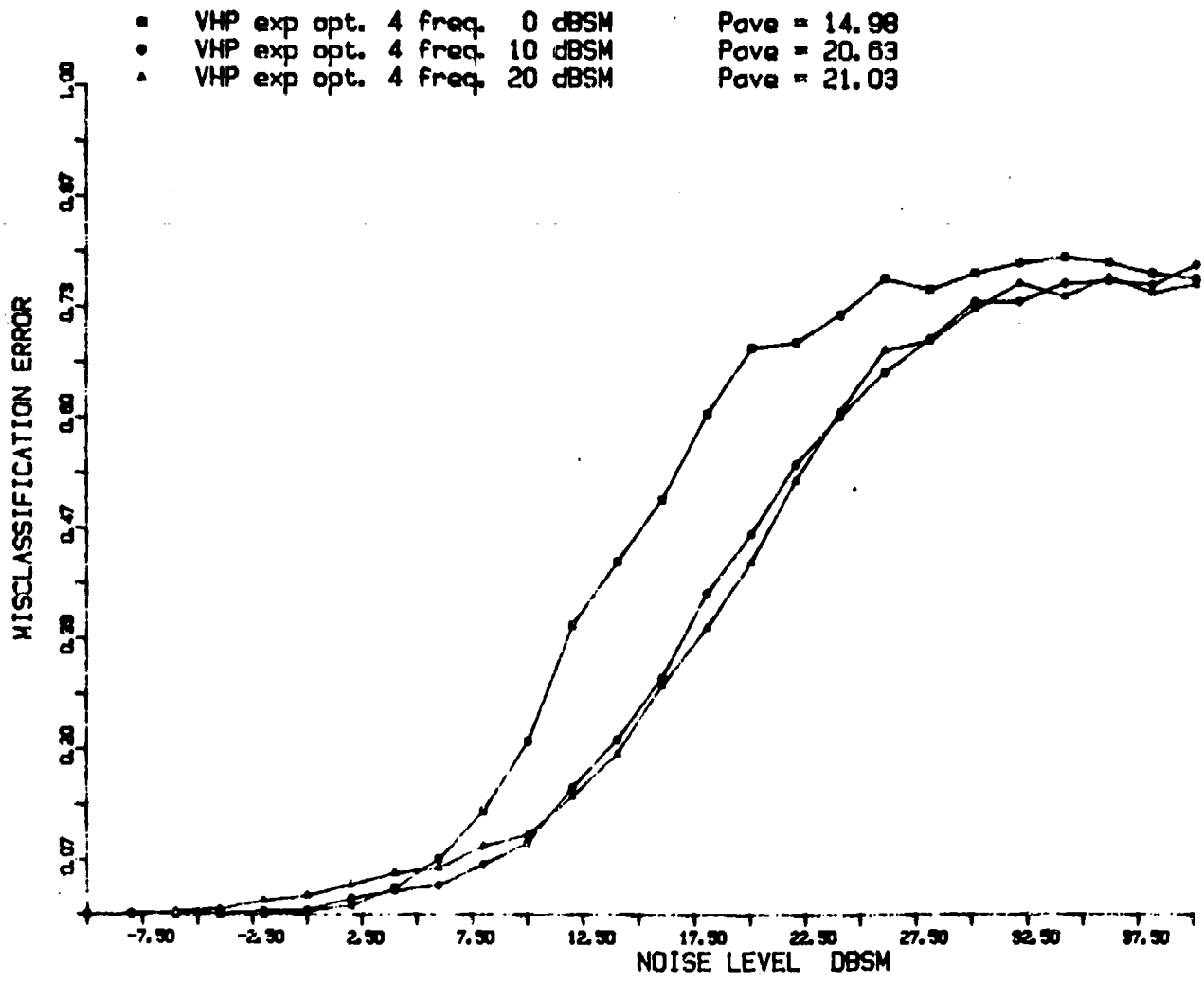

Figure 8. Misclassification error as a function of noise level (VHP catalog data).

V. TARGET SUBSTRUCTURE STUDIES

The goals of the study of scattering phenomena on this program are:

1. To identify typical scattering centers and scattering phenomena for classes of targets to be studied/identified.

2. To relate the "features" being used in the target recognition algorithms to the scattering phenomena.

3. To infer the reliability and robustness of the identification algorithm based on the behavior of the features vs. scattering phenomena as the target is moved, as clutter and noise are introduced, as target shapes are varied, and as propagation distortion is introduced.

The principal tool for the scattering phenomena study are radar target images derived from the measured transient radar target signatures at varous target orientations. It should be remembered that the signature data are significantly different than those normally used for high resolution target radar imaging.

1. The frequency bandwidth is at least a decade (10:1)

   a. Frequency dispersion of individual scattering centers is evident.

   b. The relative strength of the scattering centers changes as a function of frequency.

2. The lowest frequency extends down into the resonance region of the target signature.

3. The angular resolution of the signatures is less than normally used for high resolution images.

   a. This is partially compensated by the extremely fine down-range resolution.

4. The system is coherent, giving polarity and polarization information as well as envelope amplitude.

   a. Thus, several extra parameters may be encoded by the image.

5. Higher order scattering mechanisms have been identified in related studies, which complicate the image. Since these may be quite characteristic of the target, these are still being studied carefully.

During this research period, we have been refining the imaging tool, and using the imaging process to look at and interpret images of several targets.

A. Image Process Improvements

The biggest change was the incorporation of a Tektronix 4129 color CRT display and color hard copy unit into the (VAX) imaging system. Compared to the DEC GIGI used previously, resolution and color control are both significantly improved. Figure 9 shows the image of a conducting sphere on the new display vs. the image formally produced as shown in Figure 10.

We are still working on a variety of modes for the use of color in the images. A traditional way has been to use color to encode amplitude, as is demonstrated in Figure 9. However, the previous scheme shown in Figure 10 used color intensity to encode amplitude, and different colors (spaced approximately around the color wheel) to represent the image information for different polarizations and polarities. The thought behind this scheme is that if a scattering

center has a particular polarization response, this would produce a unique color on the image. Other possible uses of color may relate to the frequency dispersion and or polarity of the scattering centers.

The study of transient waveforms and polarimetric color images during the past research period has produced the following general conclusions regarding target identification:

1. The concept of a scattering center can be extended downward in the frequency domain to the Rayleigh region. It is proper to talk about the scattering centers in explaining the resonance region response of an object.
2. The strongest "resonance" effects on normal targets are a result of the downrange time sequence of scattering from the scattering centers of the target. Next most important are the orientation-dependent interactions between scattering centers (edge waves, creeping waves, etc.). Finally, resonances which are independent of target orientations are in general weakest. Only on very high Q (long, thin, wire-like) targets are the orientation-independent resonances strongly received.
3. For long thin targets such as ships, the time or frequency signature processing is most effective for look angles near nose-on or tail-on. Spatial image processing is most effective for near-broadside angles.
4. The scattering centers have slow, smooth variation vs. frequency, angle, and polarization. Thus, their relative importance changes for different radar sensing conditions,

leading to aspect-dependent identification processing strategies. On the other hand, the scattering centers maintain their identifying characteristics over the whole range where they are visible.

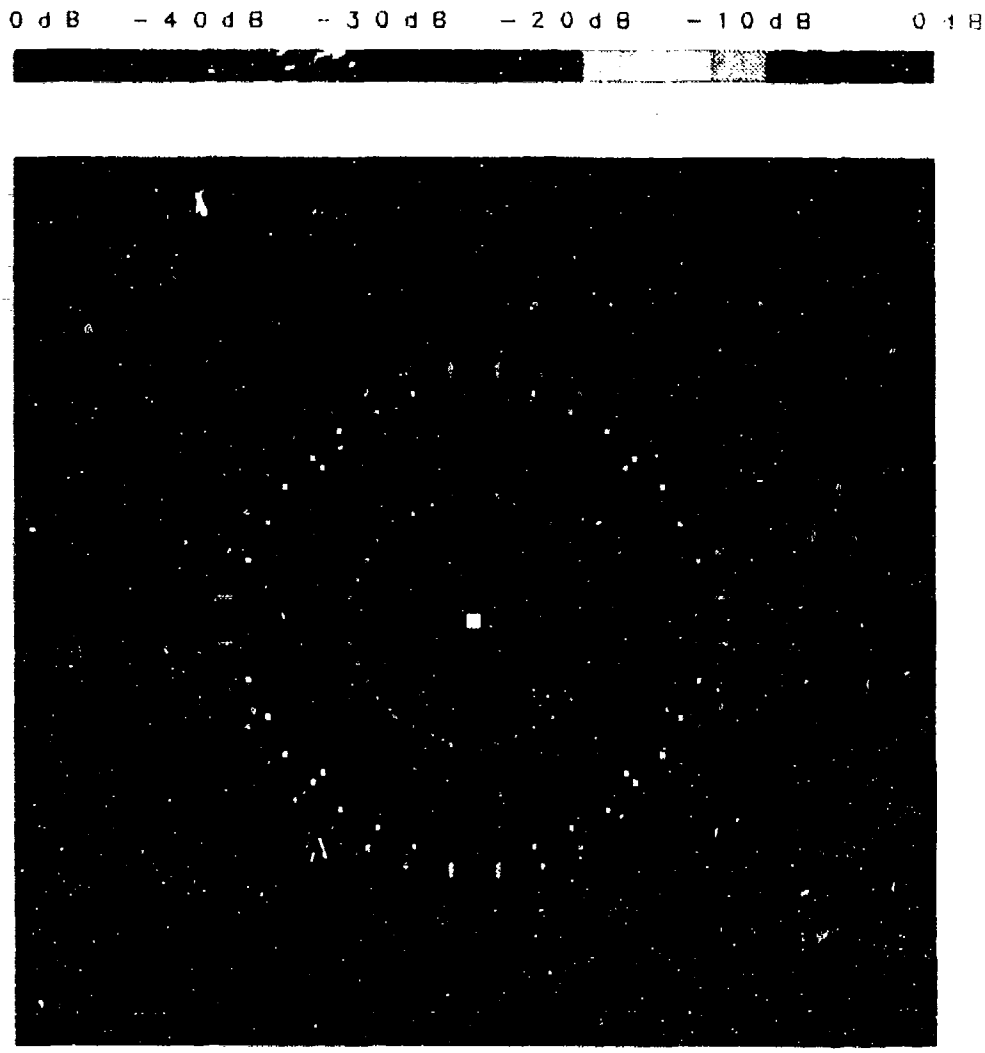

Figure 9. Conducting sphere color image on new Tektronic 4129 color display*.

*Color copies available on request

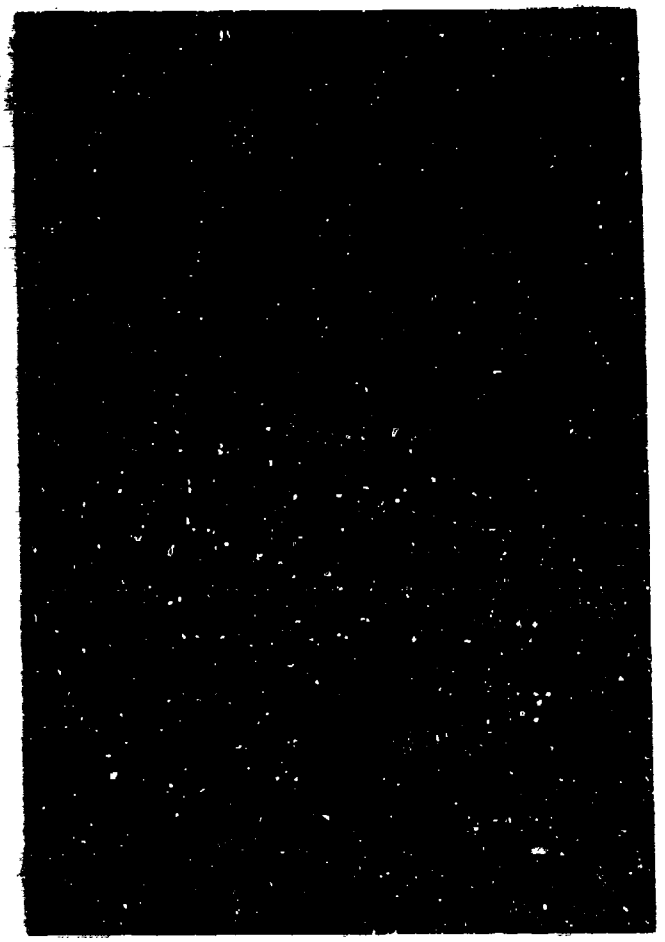

Figure 10. Conducting sphere mage on old DEC GIGI color display*.

*Color copies available on request

REFERENCES

[1] J.S. Chen and E.K. Walton, "The Ohio State University NCTR Data Base File Structure," Report 714190-1, October 1982, for Department of the Navy, Office of Naval Research, Arlington, Virginia 22217, generated under Contract No. N00014-83-K-0037.

[2] D.L. Moffatt, J.D. Young, E.K. Walton and W. Leeper, "Resonant Structure NCTR," Final Report 714190-2, January 1983, for Department of the Navy, Office of Naval Research, Arlington, Virginia 22217, generated under Contract No. N00014-83-K-0037.

[3] Jenshiun Chen, "Automatic Classification Using HF Multifrequency Radars," Report 714190-3, October 1983, for Department of the Navy, Office of Naval Research, Arlington, Virginia 22217.

[4] D.F. Kimball, "Enhanced Techniques for Broadband Radar Backscatter Measurements," Report 714190-4, December 1983, for Department of the Navy, Office of Naval Research, Arlington, Virginia 22217.

[5] S. Pleasants and M. Poirier, "A Digital Camera Systems for Non-Intrusive Measurement of Experimental Radar Test Target Position," Report 714190-5, March 1984, for Department of the Navy, Office of Naval Research, Arlington, Virginia 22217.

[6] S. Pleasants, "A Microprocessor System for Controlling the Ohio State University Compact Range Target Support Pedestal," Report 714190-6, May 1984, for Department of the Navy, Office of Naval Research, Arlington, Virginia 22217.

[7] A. Jalloul and E.K. Walton, "Aspect Scan User's Program for RCS Measurements," Report 714190-7, May 1984, for Department of the Navy, Office of Naval Research, Arlington, Virginia 22217.

[8] N.F. Chamberlain, "Surface Ship Classification Using Multipolarization, Multifrequency Sky-Wave Resonance Radar," Report 714190-9, October 1984, for Department of the Navy, Office of Naval Research, Arlington, Virginia 22217.

[9] N.F. Chamberlain, "Ground Vehicle Classification Using Multifrequency Multipolarization Resonance Radar," Report 714190-10, July 1985, for Department of the Navy, Office of Naval Research, Arlington, Virginia 22217.

[10] F.Y.S. Fok, "Space-Frequency Sampling Criteria for Electromagnetic Scattering of a Finite Object," Report 714190-11, August 1985, for Department of the Navy, Office of Naval Research, Arlington, Virginia 22217.

[11] A. Jalloul, "Discrimination of Radar Targets Using Target Complex Natural Resonances," M.Sc. thesis, The Ohio State University, Department of Electrical Engineering, Columbus, Ohio, Winter 1985.

[12] L. Marin, "Natural Mode Represenation of Transient Scattered Fields," IEEE Trans. Antennas and Propagation, Vol. AP-21, No. 6, pp. 808-819, November 1973.

[13] L.B. Felsen, "Comments on early Time SEM," IEEE Trans. Antennas and Propagation, Vol. AP-33, No. 1, pp. 118-120, January 1985.

[14] C-Y Lai, "Improved Models for the Extraction and Application of Complex Natural Resonances to Target Identification," Ph.D. dissertation, The Ohio State University, Columbus, Ohio, March 1986.

[15] D.L. Moffatt and C-Y Lai, "Natural Resonance Estimation," IEEE Trans. Instrumentation and Measurement, Vol. IM-34, No. 4, pp. 547-550, December 1985.

[16] D.L. Moffatt, "Non-Cooperative Target Recognition," a report in preparation.

[17] D.L. Moffatt and C-Y Lai, "Complex Natural Resonance Extraction from Cross-Polarized Measured Scattering Data," WAVE MOTION, 8, pp. 259-265, May 1986.

[18] J.N. Brittingham, E.K. Miller and J.L. Willows, "Pole Extraction from Real Frequency Information," Proc. IEEE, Vol. 68, No. 2, pp. 263-273, February 1980.

[19] A. Jalloul, "Discrimination of Radar Targets Using Target Complex Natural Resonances," M.Sc. thesis, The Ohio State University, Columbus, Ohio, May 1985.

[20] D.L. Moffatt and S. Barkeshli, "A Prediction-Correlation Algorithm for Recognition of Non-Cooperative Aircraft Target," NATO/AGARD Target Signature Symposium, London, England, October 1984. Paper withdrawn because of classification.

[21] E. Bohley, "A Method for Discrimination of Radar Targets Using Complex Natural Resonances," M.Sc. thesis, The Ohio State University, Columbus, Ohio, Dember 1985.

[22] F.Y.S. Fok, "K-Pulse Estimation from the Impulse Response of a Target," Ph.D. dissertation, The Ohio State University, Columbus, Ohio, June 1986.

[23] K.S. Fu, Syntactic Methods in Pattern Recognition. New York: Academic Press, 1974.

[24] Y. Cheng and S. Lu, "Waveform Correlation by Tree Matching," IEEE Transactions on Pattern Analysis and Machine Intelligence, Vol. PAMI-7, No. 3, pp. 299-305, May 1985.

[25] B.F. Logan, Jr., "Information in the Zero Crossings of Bandpass Signals," Bell System Technical Journal, Vol. 56, No. 4, pp. 487-510, April 1977.

[26] S.R. Curtis, A.V. Oppenheim, and J.S. Lim, "Signal Reconstruction from Fourier Transform Sign Information," IEEE Transactions on Acoustics, Speech and Signal Processing, Vol. ASSP-33, No. 3, pp. 643-656, June 1985.

[27] E.K. Walton, D.L. Moffatt, F.D. Garber, A. Kamis and C.Y. Lai, "NCTR Using a Polarization-Agile Coherent Radar System," Technical Report 716559-2, The Ohio State University, Department of Electrical Engineering, ElectroScience Laboratory, Columbus, Ohio, January 1986.

[28] S. Bow, Pattern Recognition, New York: Dekker, 1984.

[29] P.A. Devijver and J. Kittler, Pattern Recognition: A Statistical Approach. New York: Prentice Hall, 1982.